

# **Annex 1**

## **A1 Analysis of current publications correlating experimental site studies to structural earthquake damage**

<b>Table A1-1</b>		Comparison between site response estimation techniques and structural damage	
ARAI <i>et al.</i> (2000)		Estimation of ground motion characteristics and damage distribution in Gölcük, Turkey, based on microtremor measurements.	
<i>Earthquake</i>	<i>Investigated region</i>	<i>Site characterization</i>	<i>Scale of investigations</i>
1999 İzmit (Kocaeli) earthquake ( $M_s$ 7.8)	Gölcük (Kocaeli), Türkiye	topographical profile through an urban area	local (urban), site-specific
<i>Input data</i>			
<i>information on site and subsoil</i>		<i>information on buildings and damage</i>	
- principle stratification of subsoil		- statistically (total collapse ratio): medium-rise buildings	
<i>instrumental records of seismic ground motion</i>		<i>identification of vibrational characteristics</i>	
- microtremors along a line passing the urban area		- vibrational measurements on selected RC frame structures (5-storied)	
<i>Contents and steps of investigation</i>			
<ul style="list-style-type: none"> <li>- The effects of local site amplification are investigated in the city of Gölcük (Fig. 1), one of the most damaged towns in Northern Türkiye after the 1999 İzmit (Kocaeli) earthquake.</li> <li>- On the basis of computed H/V-ratios on microtremors (<i>HVNR</i>) recorded along a north-south profile through the urban area of Gölcük and rough information on subsoil topography, a two-dimensional subsoil profile can be generated (top of Fig. 2).</li> <li>- The heavily damaged zones of the city are compared with the H/V-ratios on microtremors (Fig. 3) as well as with simulated peak ground accelerations on the basis of the two-dimensional profile and a near-field record of the mainshock (station Yarımca YPT, bottom of Fig. 2).</li> <li>- Case-specific noise measurements were performed at two 5-storied RC frame buildings near the observation line. Both buildings had the same structural system, while one was heavily damaged and the other sustained the mainshock without any damages. Fig. 4 shows the spectral amplification curves between the top and ground floors of both buildings. The fundamental period of the undamaged structure can be estimated at 0.3 sec, while that of the damaged one is around 0.7 sec.</li> </ul>			
<i>Results</i>			
<ul style="list-style-type: none"> <li>- The calculated site response on the basis of the mainshock is consistent with the observed damage distribution.</li> <li>- Regarding the instrumental investigations at the selected RC frame buildings, resonance effects between site and structure are thought to be mainly responsible for structural damage.</li> </ul>			

<b>Table A1-1 (cont.)</b>		Comparison between site response estimation techniques and structural damage	
ARAI <i>et al.</i> (2000)		Estimation of ground motion characteristics and damage distribution in Gölcük, Turkey, based on microtremor measurements.	
<i>Earthquake</i>	<i>Investigated region</i>	<i>Site characterization</i>	<i>Scale of investigations</i>
1999 İzmit (Kocaeli) earthquake ( $M_s$ 7.8)	Gölcük (Kocaeli), Türkiye	topographical profile through an urban area	local (urban), site-specific

Illustrations

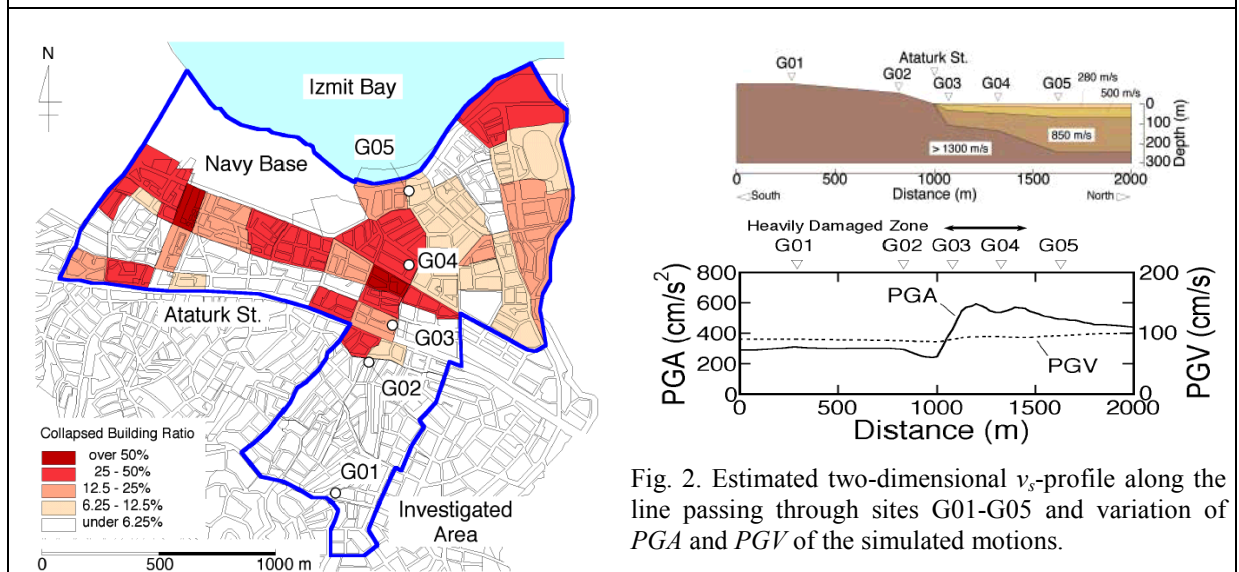


Fig. 2. Estimated two-dimensional  $v_s$ -profile along the line passing through sites G01-G05 and variation of  $PGA$  and  $PGV$  of the simulated motions.

Fig. 1. Urban map of Gölcük showing microtremor observation sites and distribution of damage to buildings.

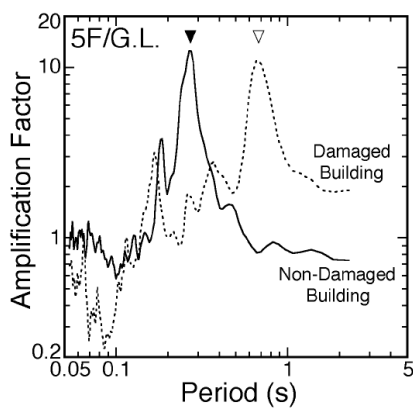


Fig. 4. Amplification factors between the top and ground floors of the damaged and the undamaged buildings.

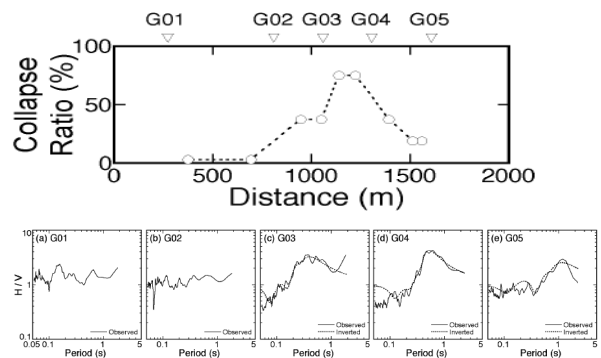


Fig. 3. Collapse ratios of medium-rise RC buildings along the observation line and H/V-spectra on microtremors compared with those theoretically computed for sites G01-G05.

<b>Table A1-2</b>		Comparison between site response estimation techniques and structural damage	
BORCHERDT <i>et al.</i> (1989)		Effects of site conditions on ground motion and damage.	
<i>Earthquake</i>	<i>Investigated region</i>	<i>Site characterization</i>	<i>Scale of investigations</i>
1988 Spitak earthquakes	Spitak, Kirovakan, Leninakan (Armenia)	basin structure (LEN), mountainous rock (KIR)	regional
<i>Input data</i>			
<i>information on site and subsoil</i>		<i>information on buildings and damage</i>	
<ul style="list-style-type: none"> <li>- geology and estimated thickness of sediments</li> <li>- detailed geological cross-sections for deposits beneath the city of Leninakan</li> </ul>		<ul style="list-style-type: none"> <li>- statistical damage analysis of:               <ul style="list-style-type: none"> <li>precast-frame (5, 9, 12-storied),</li> <li>composite-frame-stone (4, 5-storied) and</li> <li>stone (<math>\leq 4</math>-storied) buildings</li> </ul> </li> </ul>	
<i>instrumental records of seismic ground motion</i>		<i>identification of vibrational characteristics</i>	
<ul style="list-style-type: none"> <li>- aftershocks with magnitudes <math>M</math> 4.0 - 5.0</li> </ul>			
<i>Contents and steps of investigation</i>			
<ul style="list-style-type: none"> <li>- During the Spitak earthquake on December 7, 1988, the Armenian cities Spitak (<math>R_e = 1-9</math> km), Kirovakan (<math>R_e = 25</math> km), and Leninakan (<math>R_e = 32</math> km) suffered heavy structural damage. While the greater amount of the damage in Spitak can be explained by the proximity of the city to the rupture zone, an interesting observation was, that the amount of damage in Leninakan was greater than in Kirovakan, which is situated closer to the surface rupture zone.</li> <li>- A statistical damage analysis of those structural types being demolished or heavily damaged was conducted (Table 1). For the cities Leninakan and Kirovakan, the extent of occurred damage among the different building types is correlated to their average natural building period (Figure 1).</li> <li>- On the basis of numerous borehole logs around the region (see Figure 2), the subsoil conditions of both cities are well known. They can be described as follows:               <ul style="list-style-type: none"> <li><i>Leninakan</i> is located on a broad, alluvial plain within a sedimentary basin of thick alluvial sections extending to depths of 300-400 m (Fig. 3).</li> <li><i>Kirovakan</i> is situated in a mountainous region. Much of the city appears to be located on old river deposits up to a thickness of several tens of meters, while the larger proportion of the structures in Kirovakan are probably underlain by rock.</li> </ul> </li> <li>- Instrumental results are only presented for the recording stations in Leninakan. The large spectral amplifications in computed spectral ratios may be characteristic of a large proportion of the sedimentary basin beneath Leninakan. The large amplifications in the long-period range of ground motion (<math>T_s = 1.0 - 2.5</math> sec) correlate well with increased damage percentages for the longer-period structures in Leninakan.</li> </ul>			
<i>Results</i>			
<ul style="list-style-type: none"> <li>- Instrumental results are not applicable to interpreting different amounts of structural damage.</li> <li>- Though detailed information on the subsoil beneath Leninakan is available, deeper theoretical investigations are missing.</li> <li>- Neither instrumental results nor subsoil conditions are incorporated in damage interpretation.</li> </ul>			

<b>Table A1-2 (cont.)</b>	Comparison between site response estimation techniques and structural damage
---------------------------	--

BORCHERDT <i>et al.</i> (1989)	Effects of site conditions on ground motion and damage.
--------------------------------	---

<i>Earthquake</i>	<i>Investigated region</i>	<i>Site characterization</i>	<i>Scale of investigations</i>
1988 Spitak earthquakes	Spitak, Kirovakan, Leninakan (Armenia)	basin structure (LEN), mountainous rock (KIR)	regional

Illustrations

Table 1. Damage statistics for multistoried residential structures.

City	Precast-panel (5, 9 stories)		Precast-frame (5, 9, 12 stories)		Composite-frame-stone (4, 5 stories)		Stone (≤4 stories)	
	%	No.	%	No.	%	No.	%	No.
Spitak	0	1	0	0	88	9	88	25
Kirovakan	0	4	0	108	23	571	41	244
Leninakan	0	16	95	133	62	229	38	498

Note: Percentages are of structures collapsed or needing to be demolished

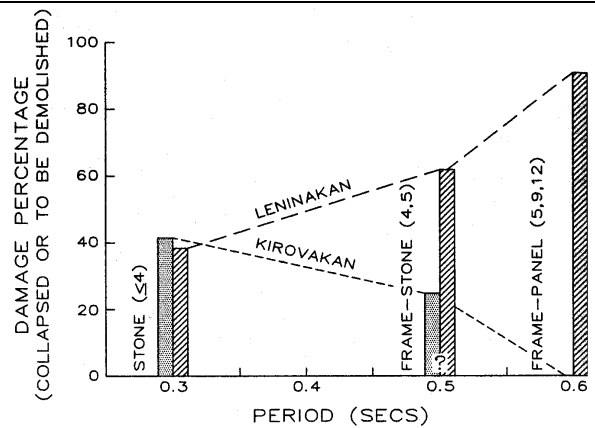


Fig. 1. Damage percentages for residential buildings that collapsed or had to be demolished in Leninakan and Kirovakan, plotted as a function of rough estimates for average building period,  $T_n$ .

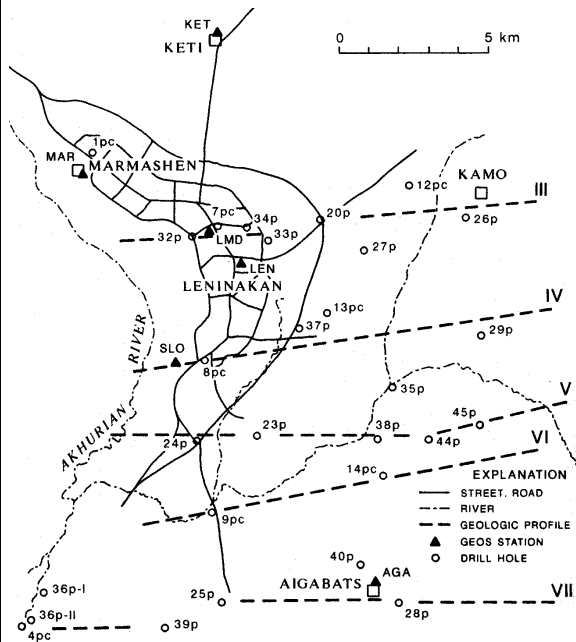


Fig. 2. Map showing geological cross-sections and recording stations in and around the city of Leninakan (Armenia).

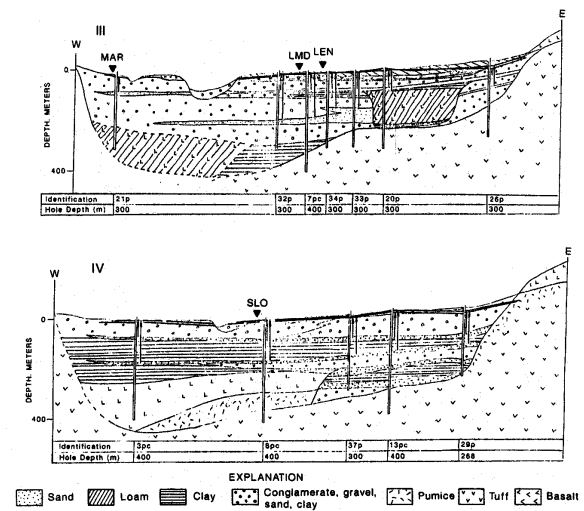
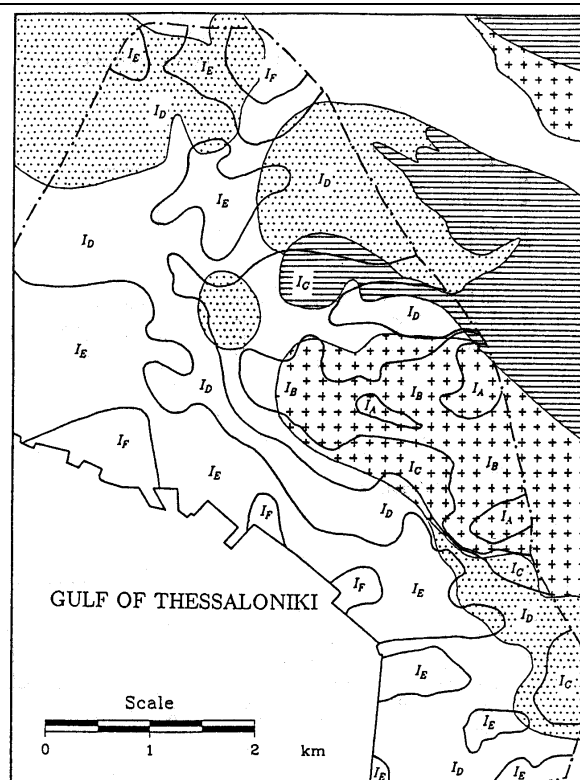


Fig. 3. Geological cross-sections for deposits beneath the city of Leninakan (derived from borehole logs as identified in Fig. 2).

<b>Table A1-3</b>		Comparison between site response estimation techniques and structural damage	
CHÁVEZ-GARCÍA <i>et al.</i> (1990)		An experimental study of the site effects near Thessaloniki (Northern Greece).	
<i>Earthquake</i> earthquake sequence of June 1978	<i>Investigated region</i> region of Thessaloniki (Greece)	<i>Site characterization</i>	<i>Scale of investigations</i> regional
<i>Input data</i>			
<i>information on site and subsoil</i> - classification of the region into 4 geological classes: 1. crystalline rocks    2. sedimentary rocks 3. neogene                4. recent deposits		<i>information on buildings and damage</i> - statistical damage analysis on the basis of macro-seismic observations	
<i>instrumental records of seismic ground motion</i> - earthquakes		<i>instrumental records of the vibrational characteristics</i>	
<i>Contents and steps of investigation</i>			
<ul style="list-style-type: none"> <li>- A detailed investigation of damage distribution was undertaken for the city of Thessaloniki (Greece) after the June 1978 earthquakes.</li> <li>- Irregular damage distribution has been ascribed to local geology, as the city's subsoil includes very different terrains. The comparison between surface geology/soil type and observed seismic intensity shows a clear overall correlation (Fig. 1).</li> <li>- The softer the subsoil materials are, the higher the observed damage intensities (Fig. 2).</li> </ul>			
<i>Results</i>			
<ul style="list-style-type: none"> <li>- The link to instrumental results of the study is very rough; spectral ratios of earthquakes (<i>SRSR</i>) show no clear correlation to these results at most of the presented recording sites.</li> <li>- An explicit interpretation of damage is not given.</li> </ul>			

<b>Table A1-3 (cont.)</b>		Comparison between site response estimation techniques and structural damage	
CHÁVEZ-GARCÍA <i>et al.</i> (1990)		An experimental study of the site effects near Thessaloniki (Northern Greece).	
<i>Earthquake</i> earthquake sequence of June 1978	<i>Investigated region</i> region of Thessaloniki (Greece)	<i>Site characterization</i>	<i>Scale of investigations</i> regional

Illustrations



- |   |                      |
|---|----------------------|
| Recent deposits. Holocene<br>Clays-Sands-Pebbles    | $I_A < 5.5$          |
| Alluvium. Neogene<br>Red clays                      | $5.5 \leq I_B < 6.0$ |
| Sedimentary rocks<br>Marls-Limestones-Quartzites    | $6.0 \leq I_C < 6.5$ |
| Crystalline rocks<br>Gneiss-Granodiorite-Ophiolites | $6.5 \leq I_D < 7.0$ |
|   | $7.5 \leq I_E$       |

Fig. 1. Geological map of the city of Thessaloniki superimposed with the intensity contours given by the analysis of damage distribution.

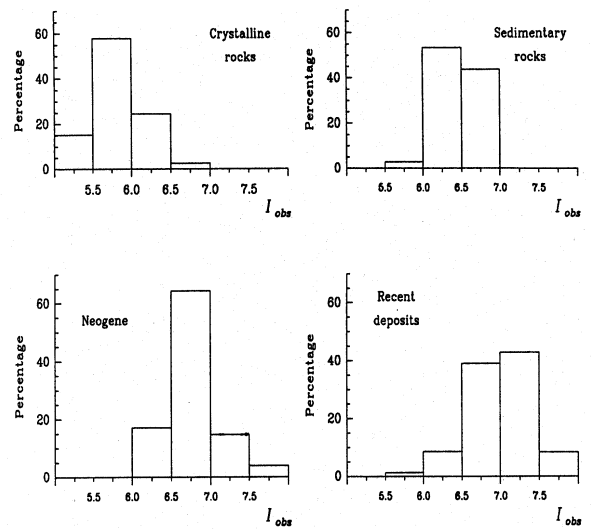


Fig. 2. Histograms of percentage of observed damage intensities in dependence on geological subsoil.

<b>Table A1-4</b>		Comparison between site response estimation techniques and structural damage	
DUVAL <i>et al.</i> (1998)		Relation between curves obtained from microtremor and site effects observed after Caracas 1967 earthquake.	
<i>Earthquake</i> 1967 Caracas, Venezuela, earthquake	<i>Investigated region</i> Caracas (Venezuela)	<i>Site characterization</i> basin structure	<i>Scale of investigations</i> local (urban)
<i>Input data</i>			
<i>information on site and subsoil</i> - stratification and subsoil parameters along a profile on the basis of seismic refraction studies and geophysical boreholes		<i>information on buildings and damage</i> - case-specific depending on the number of stories: 14 stories (high-rise buildings) 6 to 9 stories (intermediate buildings) 1 to 2 stories	
<i>instrumental records of seismic ground motion</i> - microtremors		<i>instrumental records of the vibrational characteristics</i>	
<i>Contents and steps of investigation</i>			
<ul style="list-style-type: none"> <li>- During the 1967 earthquake in Caracas, Venezuela, different types of buildings in the city were seriously damaged. While damage to high-rise buildings (&gt; 14 stories) was concentrated in <i>Palos Grandes</i> (a basin of alluvial deposits), damages to 1- and 2-storied buildings were particularly recognized in the northwestern part of Caracas, where alluvial deposits are missing. Structural damages to intermediate buildings (6-9 stories) were regularly spaced over the whole basin (Fig. 1).</li> <li>- The observed damage statistics strongly suggests a link between sediment depth and building height, indicating resonance effects between subsoil and structures.</li> <li>- On the basis of microtremor measurements conducted over the whole city area, correlations between the predominant peak frequency and the depth of sedimentary layer are established along an east-west profile (Fig. 2), as well as along a north-south profile (Fig. 3 and top of Fig. 4).</li> <li>- An overall correlation between the maximum peak amplitudes and sediment thickness cannot be observed (bottom of Fig. 4).</li> </ul>			
<i>Results</i>			
<ul style="list-style-type: none"> <li>- No explicit interpretation of damage cases is given by the authors. Resonance phenomena between site and high-rise structures (<math>f_n = 0.6</math> Hz) in the middle of the basin are briefly mentioned, but not substantiated.</li> </ul>			



<b>Table A1-4 (cont.)</b>		Comparison between site response estimation techniques and structural damage	
DUVAL <i>et al.</i> (1998)		Relation between curves obtained from microtremor and site effects observed after Caracas 1967 earthquake.	
<i>Earthquake</i>	<i>Investigated region</i>	<i>Site characterization</i>	<i>Scale of investigations</i>
1967 Caracas, Venezuela, earthquake	Caracas (Venezuela)	basin structure	local (urban)

Illustrations

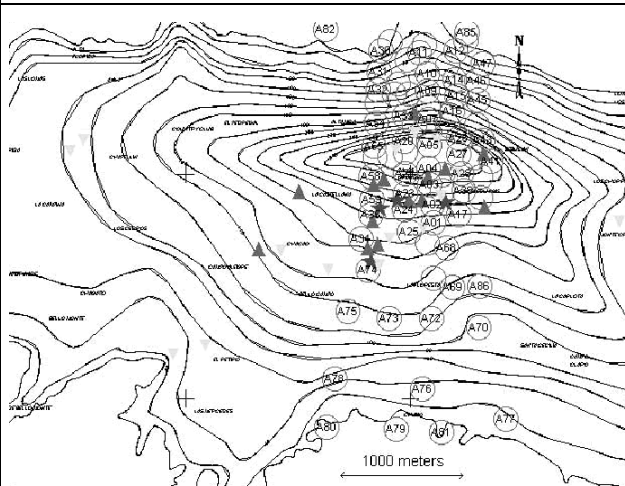


Fig. 1. Eastern part of the Caracas Basin. Level curves represent alluvium depth. Triangles and stars indicate locations of structural damage.

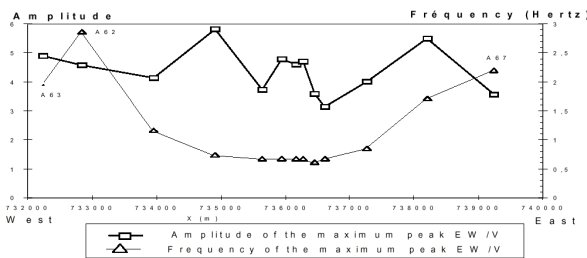


Fig. 2. Results of spectral H/V-ratios on microtremors along an east-west axis through the Caracas Basin. Squares represent the maximum value of H/V-spectra, while triangles stand for associated frequency,  $f_s$ .

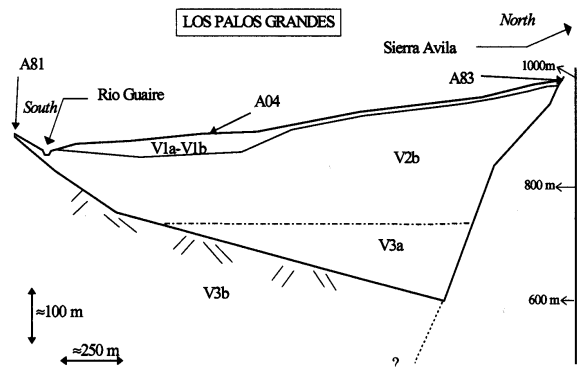


Fig. 3. North-south cross-section of the Caracas Basin with schematic stratification.

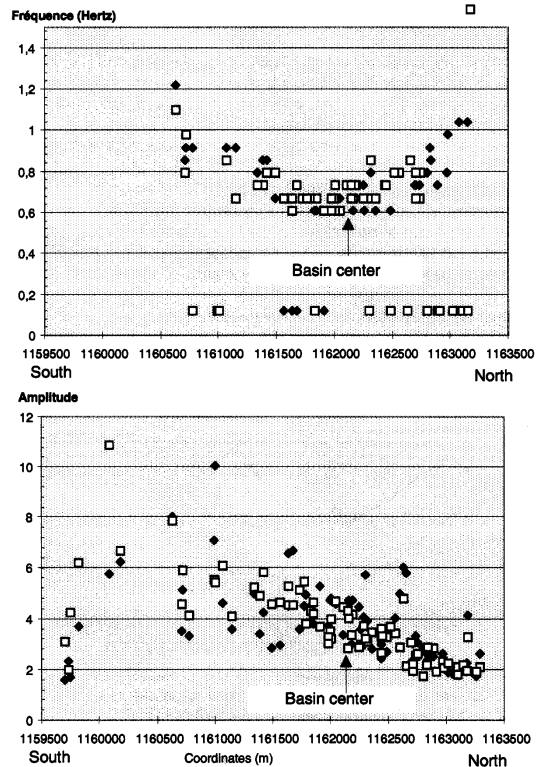


Fig. 4. Results of spectral H/V-ratios on microtremors along the north-southern profile through the basin (top: values of dominant frequency, bottom: maximum peak amplitudes).

<b>Table A1-5</b>		Comparison between site response estimation techniques and structural damage	
FIELD <i>et al.</i> (1992)		Earthquake site response estimation: A weak-motion case study.	
<i>Earthquake</i> 1989 Loma Prieta earthquake ( $M_s$ 7.1)	<i>Investigated region</i> Oakland, California (United States)	<i>Site characterization</i> bay region	<i>Scale of investigations</i> site-specific
<i>Input data</i>			
<i>information on site and subsoil</i> - dynamic parameters describing one-dimensional subsoil profiles		<i>information on buildings and damage</i> - case-specific: two segments of the Nimitz Freeway (damaged and undamaged part)	
<i>instrumental records of seismic ground motion</i> - aftershocks ( $m_b \leq 4.4$ )		<i>instrumental records of the vibrational characteristics</i>	
<i>Contents and steps of investigation</i>			
<ul style="list-style-type: none"> <li>- A segment of the Nimitz Freeway (near Oakland/U.S.) was heavily damaged during the 1989 Loma Prieta earthquake. The rest endured the seismic excitation.</li> <li>- On the basis of weak-motion recordings of aftershocks recorded at 5 sites (S1-S5) within the region, an attempt is made to interpret the different amounts of damage on the Nimitz Freeway (Fig. 1). Standard-spectral ratios of recorded earthquakes (<i>SRSR</i>) are compared with theoretical transfer functions of the one-dimensional subsoil profiles.</li> <li>- Instrumental and theoretical results (Fig. 2) of sites S1 (situated on the same subsoil as the collapsed part of the freeway) and site S3 (noncollapsed part) are correlated in respect to their extent of damage.</li> </ul>			
<i>Results</i>			
<ul style="list-style-type: none"> <li>- An explicit interpretation of the different amounts of damage is not given. Seismic amplification potential of site S1 is clearly much higher than of site S3, perhaps caused by the extremely soft mud-layer at site S1.</li> </ul>			

<b>Table A1-5 (cont.)</b>		Comparison between site response estimation techniques and structural damage	
FIELD <i>et al.</i> (1992)		Earthquake site response estimation: A weak-motion case study.	
<i>Earthquake</i>	<i>Investigated region</i>	<i>Site characterization</i>	<i>Scale of investigations</i>
1989 Loma Prieta earthquake ( $M_s$ 7.1)	Oakland, California (United States)	bay region	site-specific

Illustrations

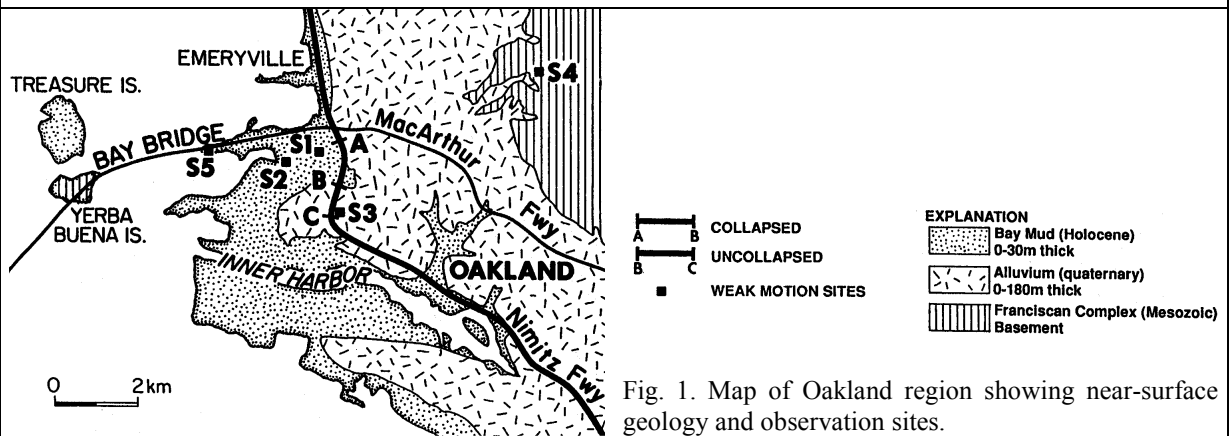


Fig. 1. Map of Oakland region showing near-surface geology and observation sites.

MUD-OVER-ALLUVIUM SITE S1.

	Thickness (m)	$\beta$ (m/sec)	$\rho$ (gm/cm <sup>3</sup> )	Q
Layer 1	6.1	90	1.6	16
Layer 2	164	384	2.0	16
Half-space	—	1,200	2.4	—

ALLUVIUM SITE S3.

	Thickness (m)	$\beta$ (m/sec)	$\rho$ (gm/cm <sup>3</sup> )	Q
Layer	159	384	2.0	16
Half-space	—	1,200	2.4	—

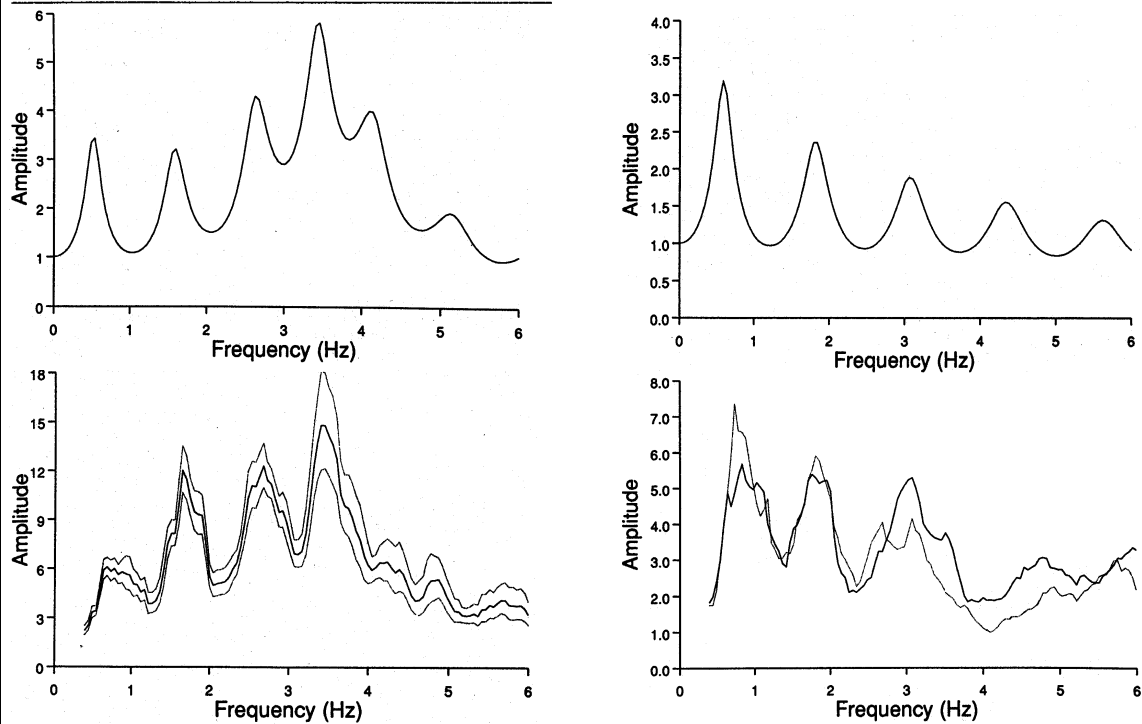


Fig. 2. One-dimensional model parameters (top), theoretical transfer function of the one-dimensional subsoil profiles (middle), and spectral ratios between the sediment sites S1 (S3) and a reference bedrock site (bottom).

<b>Table A1-6</b>		Comparison between site response estimation techniques and structural damage	
FUJIWARA <i>et al.</i> (2000)		Response characteristics of soil and structures obtained from observation networks.	
<i>Earthquake</i> 1995 Hyogo-Ken-Nanbu earthquake	<i>Investigated region</i> Kyoto City/ Hikone, Shiga (Japan)	<i>Site characterization</i>	<i>Scale of investigations</i> site-specific
<i>Input data</i>			
<i>information on site and subsoil</i> - rough information on local geology		<i>information on buildings and damage</i> - case-specific investigation of undamaged buildings: 1. DPB-building: 8-storied steel composite structure 2. USP-building: 3-storied RC structure	
<i>instrumental records of seismic ground motion</i> - earthquakes		<i>instrumental records of the vibrational characteristics</i> - microtremor records at different stories	
<i>Contents and steps of investigation</i>			
<ul style="list-style-type: none"> <li>- By using simultaneous recordings of microtremors inside and outside selected buildings in the region of Kyoto/Japan, an attempt has been made to clarify the effect of ground motion on structural behavior.</li> <li>- Two case studies are discussed in detail:               <ol style="list-style-type: none"> <li>1) The building of the Disaster Prevention Bureau in Kyoto (Fig. 1): an 8-storied steel composite structure, designed with larger values of base shear coefficients than ordinary buildings. Fundamental frequencies of this building are <math>f_n = 1.51</math> and <math>1.41</math> Hz for the <i>NS</i>- and <i>EW</i>-component, respectively. Predominant frequency of the subsoil can be estimated at <math>f_s = 6</math> Hz.</li> <li>2) The building of the University of Shiga Prefecture (Fig. 2): a 3-storied RC structure, where accelerometers are set on each floor. The observed fundamental frequencies of the building are about <math>f_n = 4.9</math> Hz in the long direction and <math>3.8</math> Hz in the short direction. The predominant frequency of subsoil <math>f_s</math> is assumed to be lower than that of DPB because of soft soil.</li> </ol> </li> <li>- Main conclusions of the authors are as follows:               <ol style="list-style-type: none"> <li>1) Response of the buildings depends on the frequency characteristics of input motion and transfer function of building structures. We must investigate in detail the reason for different amplification on similar distances from the epicenter and whether it depends on the dynamic characteristics of surface layer.</li> <li>2) Near-field earthquakes sometimes magnify the higher mode response of high-rise buildings. In order to estimate the earthquake damage in urban regions, it is necessary to predict the responses of different types of building structures not only to far-field but also to near-field earthquakes.</li> </ol> </li> </ul>			
<i>Results</i>			
<ul style="list-style-type: none"> <li>- In respect to the derived transfer functions of the sites, no clear correlation between their amplified frequency peaks and the fundamental frequency of the buildings can be observed. Moreover, differences in transfer functions of soil occur depending on the type of earthquake regarded.</li> <li>- No estimation of earthquake hazard is given for the two investigated buildings.</li> </ul>			

<b>Table A1-6 (cont.)</b>		Comparison between site response estimation techniques and structural damage	
FUJIWARA <i>et al.</i> (2000)		Response characteristics of soil and structures obtained from observation networks.	
<i>Earthquake</i>	<i>Investigated region</i>	<i>Site characterization</i>	<i>Scale of investigations</i>
1995 Hyogo-Ken-Nanbu earthquake	Kyoto City/ Hikone, Shiga (Japan)		site-specific

*Illustrations*

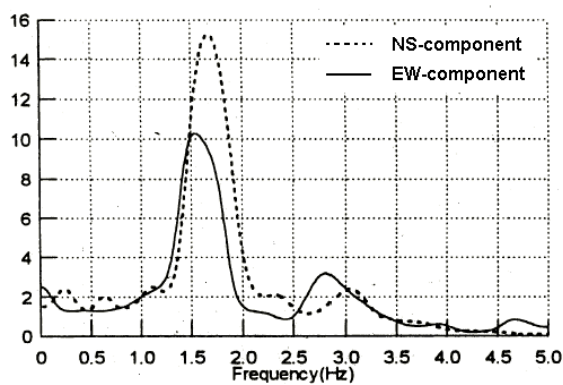
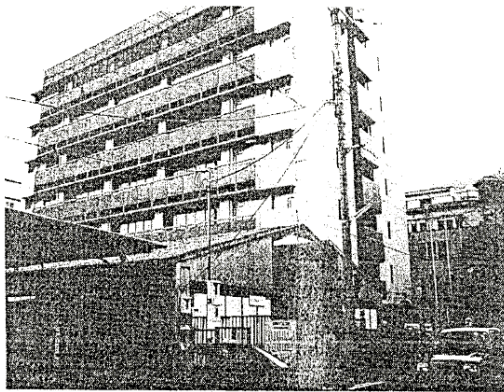


Fig. 1. View of the Disaster Prevention Bureau in Kyoto and its transfer functions of microtremors.

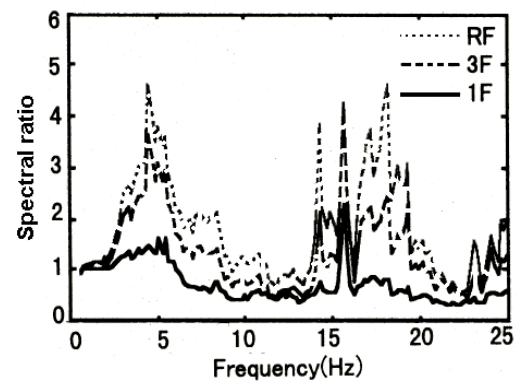


Fig. 2. View of the building of the University of Shiga Prefecture and transfer functions of microtremors.

<b>Table A1-7</b>		Comparison between site response estimation techniques and structural damage	
JONGMANS & CAMPILLO (1990)		The 1983 Liège earthquake: Damage distribution and site effects.	
<i>Earthquake</i>	<i>Investigated region</i>	<i>Site characterization</i>	<i>Scale of investigations</i>
1983 Liège earthquake	Liège (Belgium)	basin structure	local (urban)
<i>Input data</i>			
<i>information on site and subsoil</i>		<i>information on buildings and damage</i>	
<ul style="list-style-type: none"> <li>- geological information based on mining, cross-hole tests, seismic refraction, and logging</li> <li>- classification of the region into: bedrock, secondary/tertiary sediments, and recent deposits</li> </ul>		<ul style="list-style-type: none"> <li>- statistical damage analysis: damage distribution of all types of buildings</li> </ul>	
<i>instrumental records of seismic ground motion</i>		<i>instrumental records of the vibrational characteristics</i>	
<i>Contents and steps of investigation</i>			
<ul style="list-style-type: none"> <li>- An innovative approach to interpreting earthquake damage within the urban area of Liège (Belgium), which was struck by the 1983 Liège earthquake (<math>M_L</math> 4.9). The majority of the buildings in the affected region are old, 1- to 2-storied masonry houses. The worst structural damage was confined to older and poorly built structures. Modern RC frame buildings and well constructed brick dwellings were generally harmed.</li> <li>- Based on macroseismic investigations, a damage index (<math>id</math>) is calculated for each building by a weighted sum of the gravity indices that enhances the effects of the structural damages.</li> <li>- In order to point out the areas where a great number of buildings were strongly affected, a map has been created that represents the sum of damage indices. It can be shown that the extent of structural damage does not correlate with the mean age of the buildings, but rather with the presence of soft superficial deposits overlying the Carboniferous bedrock in this region (Fig. 1).</li> <li>- The main results of the study are presented in Fig. 2. Along a cross-section through the damage area, calculated site frequencies (on the basis of one-dimensional models), calculated building frequencies (using the approximate relation <math>f_n = 10/N</math>, where <math>N</math> is the number of stories), and calculated amplification factors based on different damping factors (one-dimensional model) are compared with the extent of damage (represented by damage parameter <math>IDMP</math>). Highest structural damage can be observed at sites where the site frequency, <math>f_s</math>, falls into the range of fundamental frequency of the queueing buildings, <math>f_n</math>.</li> </ul>			
<i>Results</i>			
<ul style="list-style-type: none"> <li>- Theoretical results correlate well with the amount of occurred earthquake damage. Although instrumental investigations are missing, the above method of interpreting damage is convincing.</li> </ul>			

<b>Table A1-7 (cont.)</b>		Comparison between site response estimation techniques and structural damage	
JONGMANS & CAMPILLO (1990)		The 1983 Liège earthquake: Damage distribution and site effects.	
<i>Earthquake</i>	<i>Investigated region</i>	<i>Site characterization</i>	<i>Scale of investigations</i>
1983 Liège earthquake	Liège (Belgium)	basin structure	local (urban)

Illustrations

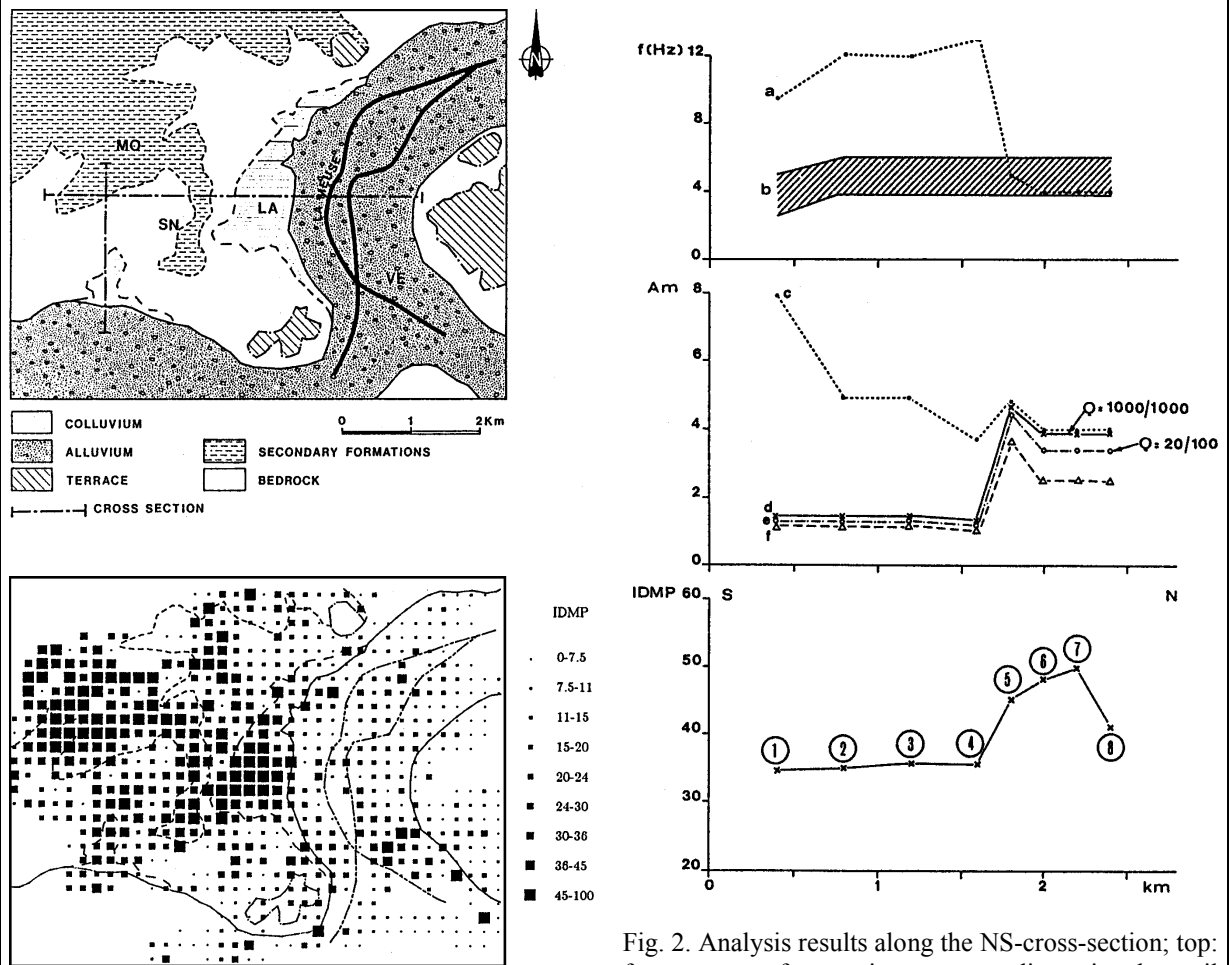


Fig. 1. Geological map of Liège with investigated cross-sections (top) and superimposed with occurrence classes of damage index IDMP (bottom).

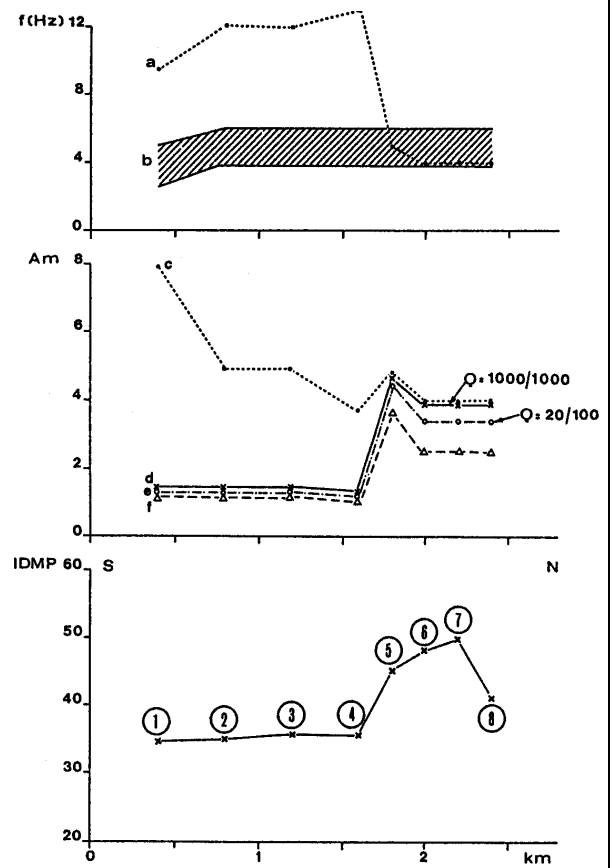


Fig. 2. Analysis results along the NS-cross-section; top: frequency of maximum one-dimensional soil amplification (a) and mean value of fundamental building's frequency (b), middle: amplification factors for different damping factors resp. seismic quality factor  $Q$  (c-f), bottom: occurrence of damage parameter IDMP.

<b>Table A1-8</b>		Comparison between site response estimation techniques and structural damage	
NAKAMURA (2000)	Clear identification of fundamental idea of Nakamura's technique and its applications.		
<i>Earthquake</i> 1989 Loma Prieta earthquake ( $M_s$ 7.1)	<i>Investigated region</i> Marina District, San Francisco (U.S.)	<i>Site characterization</i> coastline	<i>Scale of investigations</i> local (urban)
<i>Input data</i>			
<i>information on site and subsoil</i>		<i>information on buildings and damage</i> - statistical damage analysis: occurrence of earthquake damage along the coastline of San Francisco	
<i>instrumental records of seismic ground motion</i> - microtremors		<i>instrumental records of the vibrational characteristics</i>	
<i>Contents and steps of investigation</i>			
<ul style="list-style-type: none"> <li>- The dimension of structural earthquake damage depends on such parameters as strength, period, and duration of seismic ground motion, all of which are strongly influenced by seismic response characteristics of the ground's surface and structures. For this reason, the investigation of vulnerability of the ground is an important issue. This can be achieved by comparing vulnerability index of ground <math>K_g</math> with the damage grade.</li> <li>- In order to calculate damage index <math>K_g</math>, shear strain of the ground must be considered. The larger the seismic displacement and amplification factor <math>A_g</math> are, the larger the index <math>K_g</math> seems to be.</li> <li>- The spectral H/V-ratios of a considered site are used to calculate the vulnerability index <math>K_g</math>, by:  <math display="block">K_g = A_g^2 / F_g \quad \text{where:} \quad \begin{array}{ll} A_g &amp; \text{- amplitude of the predominant peak} \\ F_g &amp; \text{- predominant frequency} \end{array}</math> </li> <li>- <math>K_g</math> can be considered a vulnerability index of the site, which might be useful in selecting weak points of the ground. <math>K_g</math> is believed to be closely related to the occurrence of earthquake damage (see Fig. 2).</li> <li>- The main concluding remark can be quoted as follows: "Vulnerability index for ground <math>K_g</math> gives a chance to estimate the earthquake damage before the earthquake occurs."</li> </ul>			
<i>Results</i>			
<ul style="list-style-type: none"> <li>- Theoretical explanation of a new index establishing the link between site conditions and structural damage.</li> <li>- The presented example of damage interpretation within Marina District is only approximate.</li> </ul>			



<b>Table A1-8 (cont.)</b>		Comparison between site response estimation techniques and structural damage	
NAKAMURA (2000)		Clear identification of fundamental idea of Nakamura's technique and its applications.	
<i>Earthquake</i> 1989 Loma Prieta earthquake ( $M_s$ 7.1)	<i>Investigated region</i> Marina District, San Francisco (U.S.)	<i>Site characterization</i> coastline	<i>Scale of investigations</i> local (urban)

*Illustrations*

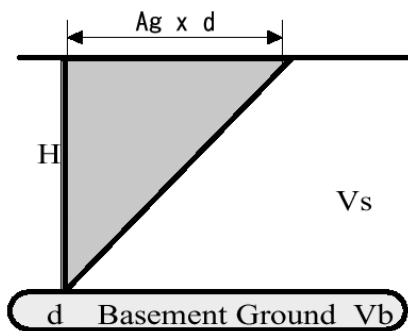


Fig. 1. Sketch illustrating surface ground deformation, where  $A_g$  is amplification factor of surface layer and  $d$  is seismic displacement of the basement.

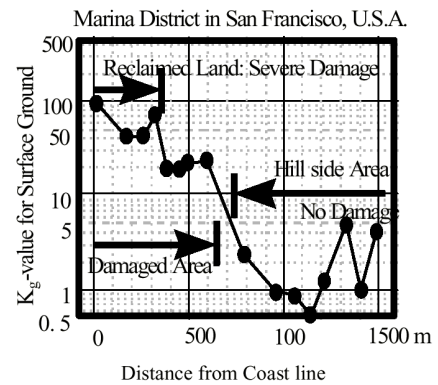


Fig. 2.  $K_g$ -values based on damage assessment after the 1989 Loma Prieta earthquake.

<b>Table A1-9</b>		Comparison between site response estimation techniques and structural damage	
NAKAMURA <i>et al.</i> (2000)		Local site effect of Kobe based on microtremor measurement.	
<i>Earthquake</i> 1995 Hyogo-Ken-Nanbu earthquake	<i>Investigated region</i> Kobe City (Japan)	<i>Site characterization</i> coastline	<i>Scale of investigations</i> local (urban)
<i>Input data</i>			
<i>information on site and subsoil</i> - liquefaction-induced region		<i>information on buildings and damage</i> - statistical damage analysis: damage ratio of small-scale structures along the coastline of Kobe City	
<i>instrumental records of seismic ground motion</i> - microtremors		<i>instrumental records of the vibrational characteristics</i>	
<i>Contents and steps of investigation</i>			
<ul style="list-style-type: none"> <li>- The 1995 Hyogo-Ken-Nanbu earthquake caused heavy damage to the city of Kobe (Japan) and to its surrounding areas.</li> <li>- Based on microtremor measurements carried out within the urban damage area and the calculation of spectral H/V-ratios (<i>HVNR</i>), an attempt to associate computed vulnerability indexes <math>K_g</math> with the amount of structural damage was made.</li> <li>- Since the comparison between the predominant frequency, <math>F</math>, and the extent of structural damage is not sufficient (left of Fig. 1), vulnerability indexes <math>K_g</math> are calculated by using the relationship of <math>F</math> and <math>A</math> (right of Fig. 1).</li> <li>- Fig. 2 compares <math>K_g</math>-value and damage ratio for small-scale structures, where damage ratio is divided into 5 ranges: 1: no damage; 2: 0 – 12.5 %; 3: 12.5 – 25 %; 4: 25 – 50%; 5: 50 – 100%</li> <li>- <math>K_g</math>-values of Fig. 2 do not agree with the damage ratio in all cases. Despite the small damage ratio, sites with large <math>K_g</math>-values are almost all located in liquefaction areas.</li> </ul>			
<i>Results</i>			
<ul style="list-style-type: none"> <li>- Practical application of vulnerability index <math>K_g</math>.</li> <li>- Although values of vulnerability indexes strongly agree with the grade of damage, a final verification of subsoil conditions is missing.</li> </ul>			

<b>Table A1-9 (cont.)</b>		Comparison between site response estimation techniques and structural damage	
NAKAMURA <i>et al.</i> (2000)		Local site effect of Kobe based on microtremor measurement.	
<i>Earthquake</i>	<i>Investigated region</i>	<i>Site characterization</i>	<i>Scale of investigations</i>
1995 Hyogo-Ken-Nanbu earthquake	Kobe City (Japan)	coastline	local (urban)

Illustrations

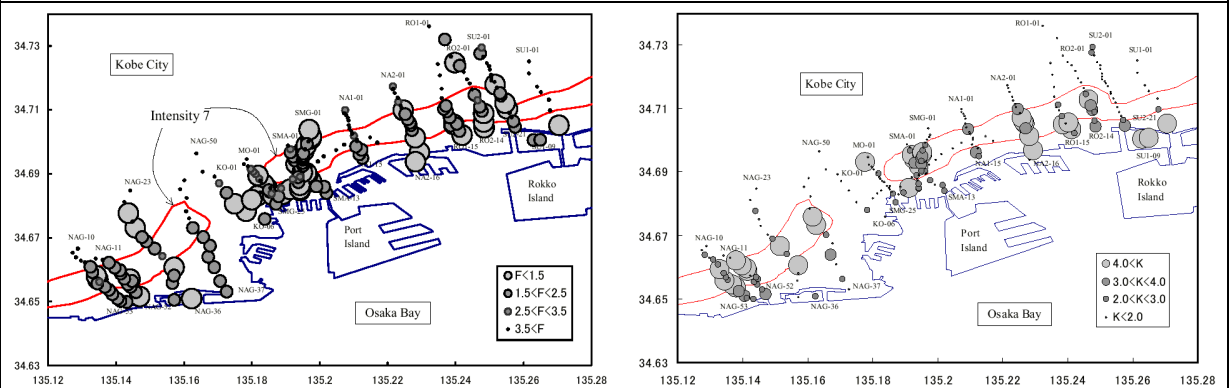


Fig. 1. Distribution of predominant frequency (left) and vulnerability index  $K_g$  (right) along the bay area of Kobe City. The highlighted area of the seismic intensity of 7 (Japanese scale) does not show the same trend as the predominant frequency,  $F$ .

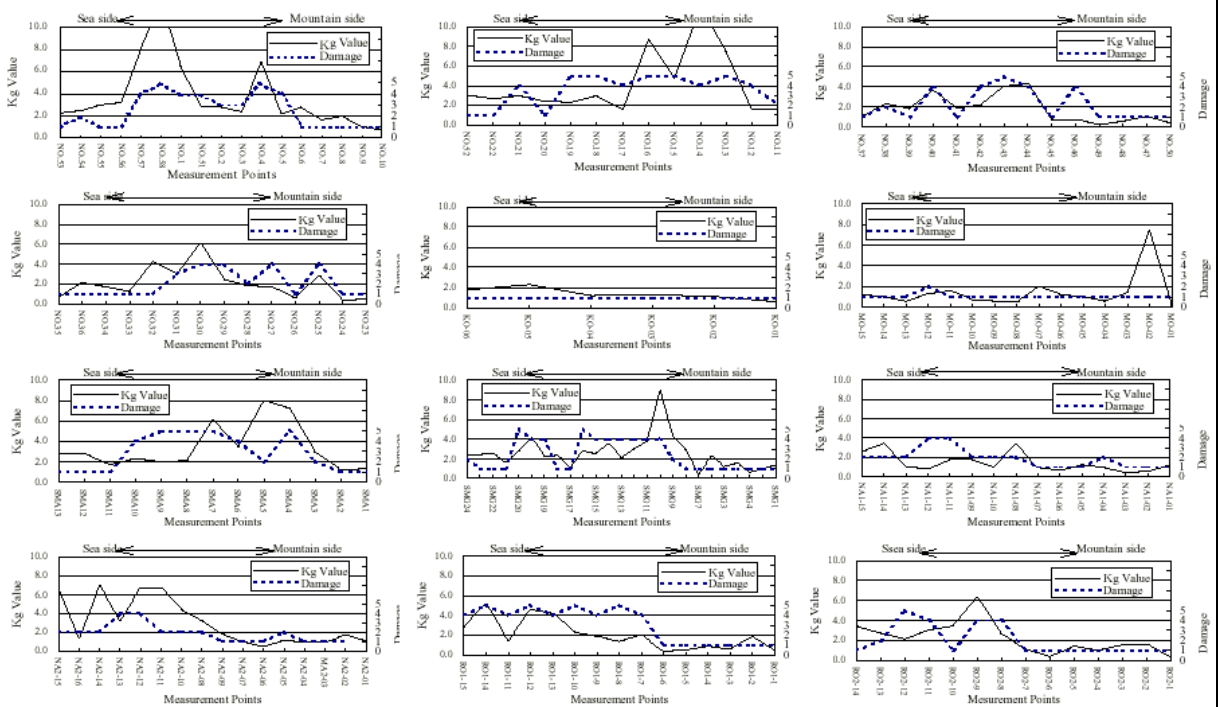


Fig. 2. Comparison between vulnerability index  $K_g$  and damage ratio for small-scale structures along the different investigation profiles perpendicular to the shoreline.

<b>Table A1-10</b>		Comparison between site response estimation techniques and structural damage	
OHMACHI <i>et al.</i> (1991a)		Ground motion characteristics with reference to damage by the Philippine earthquake of July 16, 1990.	
<i>Earthquake</i> 1990 Philippine earthquake	<i>Investigated region</i> Baguio City (Philippines)	<i>Site characterization</i> mountainous region (topographical effects)	<i>Scale of investigations</i> local (urban)
<i>Input data</i>			
<i>information on site and subsoil</i>		<i>information on buildings and damage</i> - case-specific damage analysis: all damage cases of the city are individually observed	
<i>instrumental records of seismic ground motion</i> - microtremors		<i>instrumental records of the vibrational characteristics</i>	
<i>Contents and steps of investigation</i>			
<ul style="list-style-type: none"> <li>- The paper deals with structural damage in Baguio City, caused by the 1990 Philippine earthquake.</li> <li>- Many multistoried, reinforced-concrete buildings collapsed or suffered serious damage, although such structural deficiencies as insufficient reinforcement in columns and imperfect connections between beams and columns were thought to be mainly responsible for the damage.</li> <li>- Topographical effects may also contribute to the extent of damage, as many severely damaged structures were located on hilltops and steep slopes. In order to investigate the influence of site effects on structural damage, microtremor measurements were conducted for the whole city area.</li> <li>- Fig. 1 shows a bird's-eye view of one part of the city and indicates damaged buildings as well as the recording sites of microtremors. The comparison between the results of spectral H/V-ratios, that is predominant frequency (here: <i>FREQ.</i>) and amplification factor (here: <i>AMP.FAC.</i>), and elevation of each recording station (here: <i>DIF.ELEV.</i>) shows no definite dependence on each other (Fig. 3).</li> <li>- The investigation of predominant site and building frequencies depending on the number of stories of the (nearest) building also illustrates only rough correlations (Fig. 2).</li> </ul>			
<i>Results</i>			
<ul style="list-style-type: none"> <li>- The presented instrumental results cannot be used to interpret any damage to buildings. Even the comparison between the frequency of sites where structural damage occurred and the fundamental frequencies of the damaged buildings shows no clear agreement.</li> </ul>			

<b>Table A.1-10 (cont.)</b>		Comparison between site response estimation techniques and structural damage	
OHMACHI <i>et al.</i> (1991a)		Ground motion characteristics with reference to damage by the Philippine earthquake of July 16, 1990.	
<i>Earthquake</i>	<i>Investigated region</i>	<i>Site characterization</i>	<i>Scale of investigations</i>
1990 Philippine earthquake	Baguio City (Philippines)	mountainous region (topographical effects)	local (urban)

Illustrations

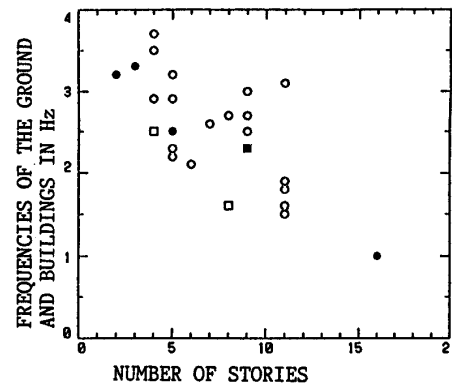
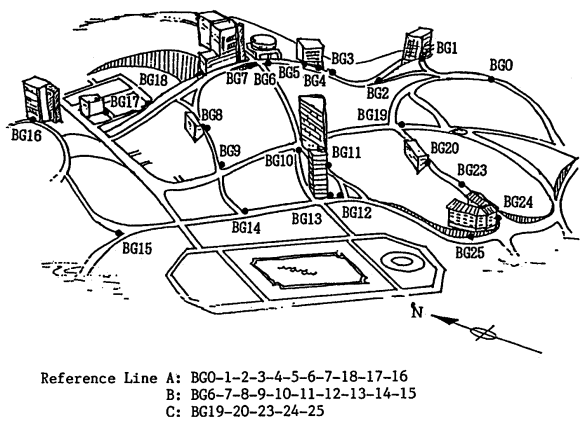


Fig. 1. Bird's-eye view of a part of Baguio City with observation sites and seriously damaged buildings.

Fig. 2. Predominant site frequencies (empty marks) and fundamental frequencies of queueing buildings (filled marks) depending on the number of stories.

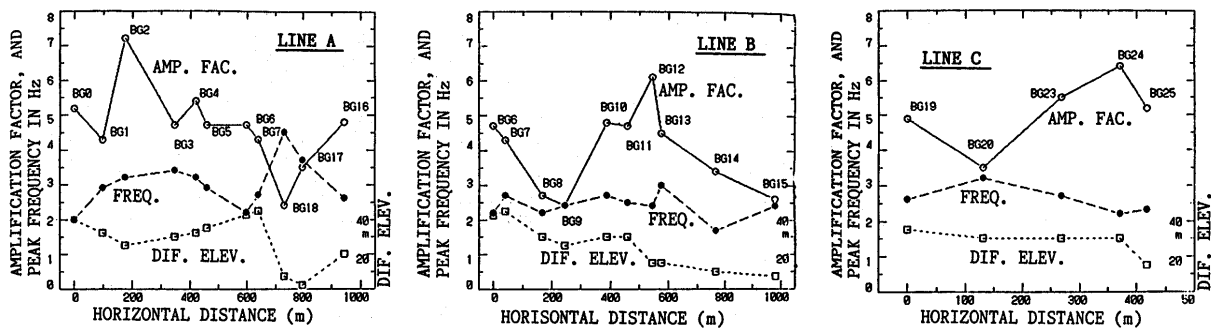


Fig. 3. Maximum amplification factors, predominant site frequencies, and differences in elevation along the observation lines A, B, C.

<b>Table A1-11</b>		Comparison between site response estimation techniques and structural damage	
OHMACHI <i>et al.</i> (1991b)		Ground motion characteristics of San Francisco Bay Area detected by microtremor measurements.	
<i>Earthquake</i>	<i>Investigated region</i>	<i>Site characterization</i>	<i>Scale of investigations</i>
1989 Loma Prieta earthquake	San Francisco, California (U.S.)	bay region	local (urban)
<i>Input data</i>			
<i>information on site and subsoil</i>		<i>information on buildings and damage</i>	
		<ul style="list-style-type: none"> <li>- statistical damage analysis: <ul style="list-style-type: none"> <li>- along different profiles through the city</li> <li>- assessment of “ranks of damage”: A, B, C</li> </ul> </li> </ul>	
<i>instrumental records of seismic ground motion</i>		<i>instrumental records of the vibrational characteristics</i>	
- microtremors			
<i>Contents and steps of investigation</i>			
<ul style="list-style-type: none"> <li>- The damaged area of San Francisco/California after the 1989 Loma Prieta earthquake was observed by grid measurements of microtremors (Fig. 1).</li> <li>- By applying spectral H/V-method on microtremors (<i>HVNR</i>), predominant frequencies and amplification factors are correlated with “ranks of damage”, which are estimated in the vicinity of the different recording stations (Table 1).</li> <li>- The main conclusions which can be drawn from the investigation are as follows: <ol style="list-style-type: none"> <li>(1) In the Marina District and South of Market, the high rank of damage strongly coincides with the large amplification factor.</li> <li>(2) Structural difference might affect the degree of damage in the Cypress and Embarcadero Viaducts.</li> <li>(3) The derived values of the amplification factor and predominant frequency may correlate with local subsoil conditions.</li> </ol> </li> </ul>			
<i>Results</i>			
<ul style="list-style-type: none"> <li>- Interpretation of structural damage is performed without implying natural frequencies of subsoil. Only the amplification factors of H/V-ratios (<i>HVNR</i>) are compared to the extent of damage.</li> </ul>			

<b>Table A1-11 (cont.)</b>	Comparison between site response estimation techniques and structural damage		
OHMACHI <i>et al.</i> (1991b)	Ground motion characteristics of San Francisco Bay Area detected by microtremor measurements.		
<i>Earthquake</i> 1989 Loma Prieta earthquake	<i>Investigated region</i> San Francisco, California (U.S.)	<i>Site characterization</i> bay region	<i>Scale of investigations</i> local (urban)

### Illustrations

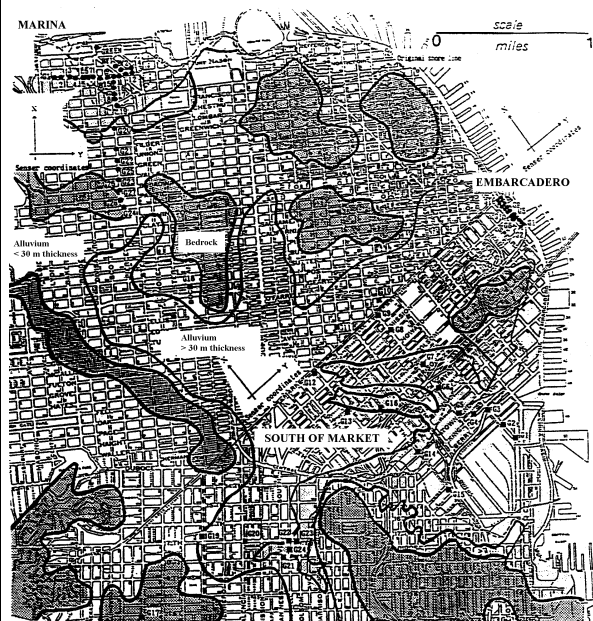


Table 1. Predominant frequencies and amplification factors compared with rank of damage of the different districts.

	$F_p$ [Hz]	$A_p$	Rank of damage*
<b>Marina</b>			
MG1-MG4	1.0 - 1.2	4 - 5	B
MG5-MG19	0.8 - 1.0	5 - 9	A
MG20-MG28	> 3.0	2 - 3	C
<b>Cypress</b>			
P87-P73	0.6 - 1.0	3.7 - 6.2	A (HT)**
	0.6 - 0.9	2.8 - 4.5	A (HL)***
P62, P61	0.7	3.7, 2.7	C (HT)
	0.7	4.4, 3.0	C (HL)
<b>Embarcadero</b>			
EG1-EG18	0.7 - 1.5	9 - 16	B (HT)
	0.7 - 1.6	9 - 16	B (HL)
<b>South of Market</b>			
SG1-SG5	0.8 - 1.6	4 - 8	B
SG14, SG15	0.8 - 1.6	4 - 8	B
SG7-SG16	1.0 - 2.8	2 - 7	C
SG19-SG23	1.5 - 2.5	2 - 7	B
SG24	1.5 - 2.5	20	A

\*Rank of damage: A - severely damaged  
B - damaged  
C - slightly or hardly damaged

\*\* HT: in the transverse direction of the "Cypress Viaduct"

\*\*\* HL: in the longitudinal direction of the "Cypress Viaduct"

Fig. 1. Map of San Francisco with subsoil geology and points of observation.

<b>Table A1-12</b>		Comparison between site response estimation techniques and structural damage	
ÖZEL <i>et al.</i> (2002)		Site effects in Avcilar, west of Istanbul, Turkey, from strong- and weak-motion data.	
<i>Earthquake</i> 1999 İzmit (Kocaeli) earthquake	<i>Investigated region</i> Avcilar, west of İstanbul (Türkiye)	<i>Site characterization</i> basin structure	<i>Scale of investigations</i> regional
<i>Input data</i>			
<i>information on site and subsoil</i> - surface geology		<i>information on buildings and damage</i> - case-specific damage analysis of RC frame structures	
<i>instrumental records of seismic ground motion</i> - microtremors (application of <i>HVNR</i> ) - aftershocks (application of <i>HVSR</i> )		<i>instrumental records of the vibrational characteristics</i> - microtremor measurements at the base and the top of 5- to 6-storied buildings	
<i>Contents and steps of investigation</i>			
<ul style="list-style-type: none"> <li>- In order to investigate the damage-provoking effects in Avcilar, west of İstanbul (Türkiye), after the 1999 İzmit (Kocaeli) earthquake, site response studies were performed at sites with different geological conditions (Fig. 1).</li> <li>- The site frequencies at selected free-field recording stations, identified by the use of H/V-spectral ratio method on earthquake recordings, are correlated to the frequency ranges of a heavily damaged building type. Spectral ratios, based on the application of standard spectral ratio technique (SRSR) on weak earthquakes, are compared with instrumentally determined building response (Fig. 2).</li> </ul>			
<i>Results</i>			
<ul style="list-style-type: none"> <li>- Investigations were only carried out at one structure, judged to be representative for the whole building type.</li> <li>- The correlation between fundamental frequency of the building and site frequency is only rough and cannot be used as an indicator for resonance effects at this stage of analysis.</li> </ul>			



<b>Table A1 -12 (cont.)</b>		Comparison between site response estimation techniques and structural damage	
ÖZEL <i>et al.</i> (2002)		Site effects in Avcilar, west of Istanbul, Turkey, from strong- and weak-motion data.	
<i>Earthquake</i>	<i>Investigated region</i>	<i>Site characterization</i>	<i>Scale of investigations</i>
1999 İzmit (Kocaeli) earthquake	Avcilar, west of İstanbul (Türkiye)	basin structure	regional

Illustrations

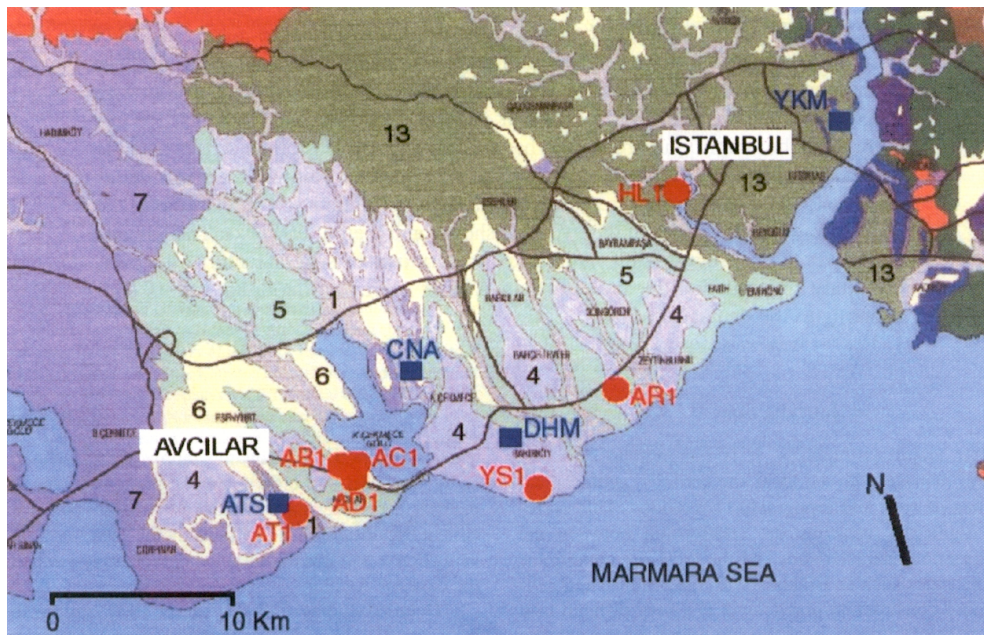


Fig. 1. Geotechnical bearing capacity map of Avcilar and western İstanbul with investigated recording sites.

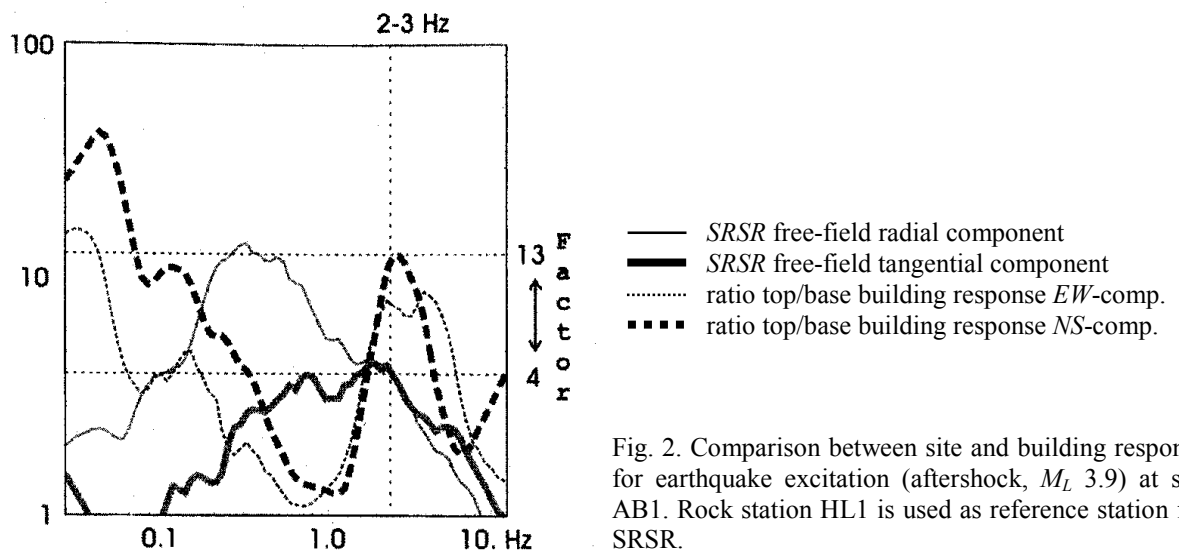


Fig. 2. Comparison between site and building response for earthquake excitation (aftershock,  $M_L$  3.9) at site AB1. Rock station HL1 is used as reference station for SRSR.

<b>Table A1-13</b>		Comparison between site response estimation techniques and structural damage	
SEO <i>et al.</i> (2000)	A joint research on microtremors in Fukui Basin, Japan - for site effects evaluation during the 1948 Fukui (Japan) earthquake.		
<i>Earthquake</i> 1948 Fukui earthquake	<i>Investigated region</i> Fukui Basin (Japan)	<i>Site characterization</i> basin structure	<i>Scale of investigations</i> regional
<i>Input data</i>			
<i>information on site and subsoil</i> - surface geology		<i>information on buildings and damage</i> - statistical damage analysis based on macroseismic observations (damage ratio)	
<i>instrumental records of seismic ground motion</i> - microtremors		<i>instrumental records of the vibrational characteristics</i>	
<i>Contents and steps of investigation</i>			
<ul style="list-style-type: none"> <li>- For the Fukui Basin region in Japan the damage ratio of totally collapsed buildings due to the 1948 Fukui earthquake is compared with local geological conditions (Fig. 1).</li> <li>- Within the basin, the ratio of totally collapsed houses ranged from 60 to 100%, while a sudden decrease of the damage ratio appeared just on the border between basin and surrounding mountains. Outside the basin there were no collapsed houses at all.</li> <li>- By presenting the shapes of spectral H/V-ratios for two recording stations inside and outside the sedimentary basin, an attempt is made to interpret the different amounts of damage (Fig. 2).</li> </ul>			
<i>Results</i>			
<ul style="list-style-type: none"> <li>- The illustrated H/V-ratios on microtremors for the two sites clearly identify the different subsoil conditions. It is also unclear whether these stations are representative for their corresponding zone of equal damage ratio.</li> <li>- Information on the types or stories of the damaged buildings is withheld.</li> </ul>			

<b>Table A1-13 (cont.)</b>		Comparison between site response estimation techniques and structural damage	
SEO <i>et al.</i> (2000)		A joint research on microtremors in Fukui Basin, Japan - for site effects evaluation during the 1948 Fukui (Japan) earthquake.	
<i>Earthquake</i>	<i>Investigated region</i>	<i>Site characterization</i>	<i>Scale of investigations</i>
1948 Fukui earthquake	Fukui Basin (Japan)	basin structure	regional

Illustrations

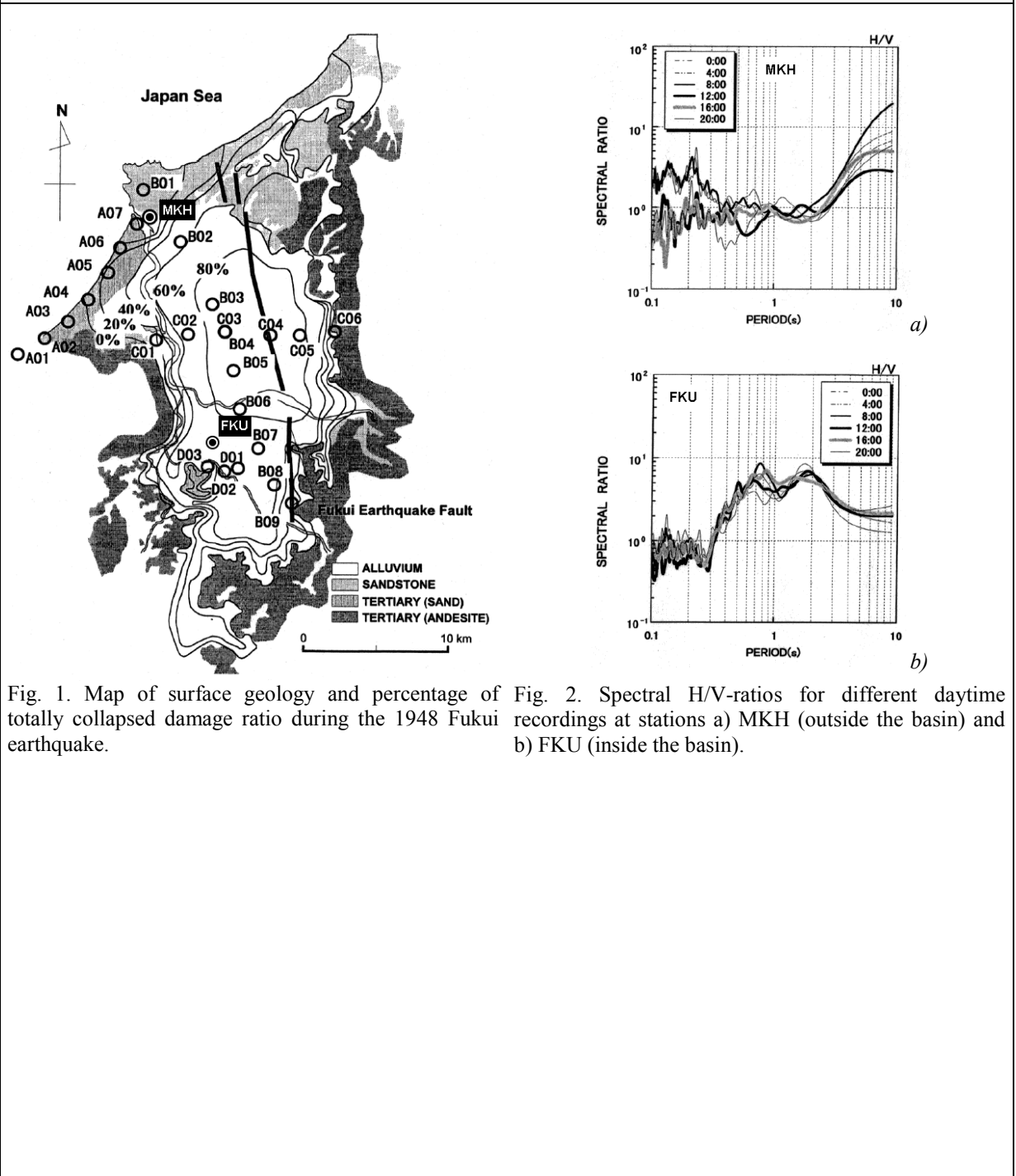


Fig. 1. Map of surface geology and percentage of totally collapsed damage ratio during the 1948 Fukui earthquake.

Fig. 2. Spectral H/V-ratios for different daytime recordings at stations a) MKH (outside the basin) and b) FKU (inside the basin).